

Supporting Information

**Three-Dimensional Double-Walled Ultrathin Graphite Tube Conductive Scaffold with Encapsulated Germanium Nanoparticles as a High-Areal-Capacity and Cycle-Stable Anode for Lithium-Ion Battery**

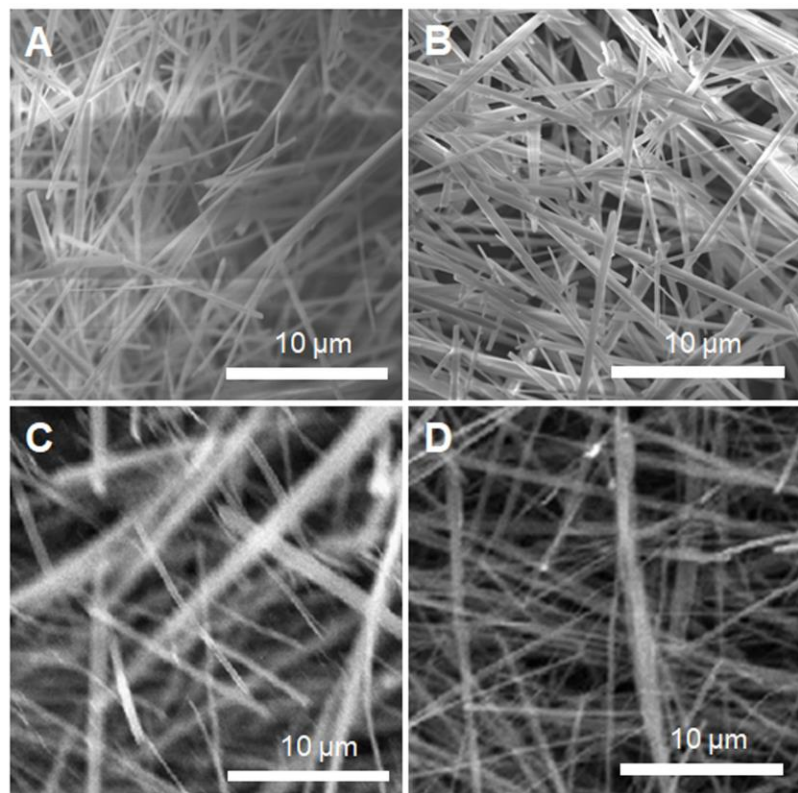
Runwei Mo<sup>1#\*</sup>, Zhengyu Lei<sup>1#</sup>, David Rooney<sup>2</sup>, Kening Sun<sup>1\*</sup>

1 Academy of Fundamental and Interdisciplinary Sciences, Harbin Institute of Technology, Harbin 150001, (China)

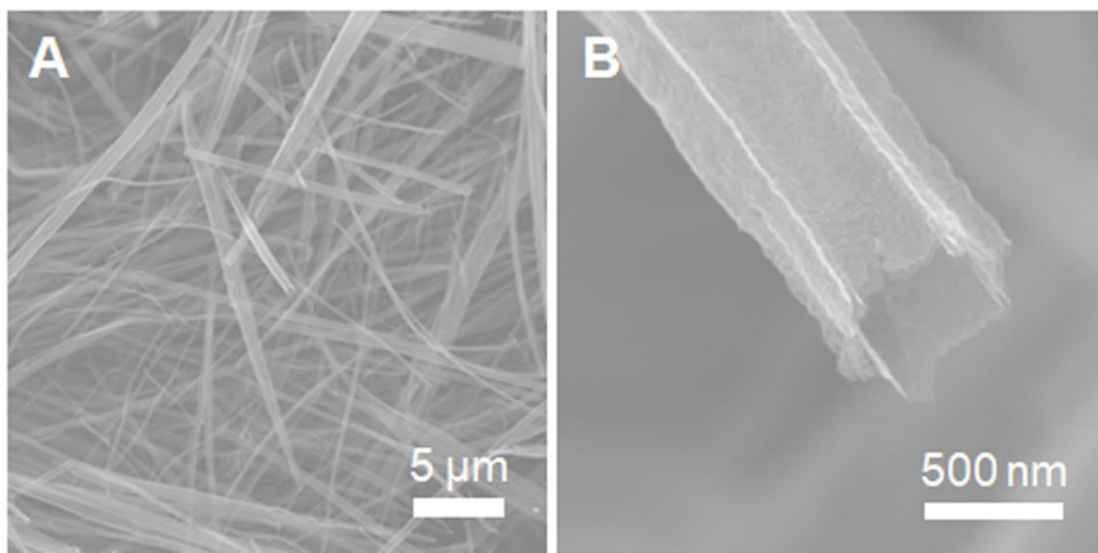
2 School of Chemistry and Chemical Engineering, Queen's University Belfast, Belfast, BT9 5AG, (Northern Ireland)

# R.M. and Z.L. contributed equally to this work.

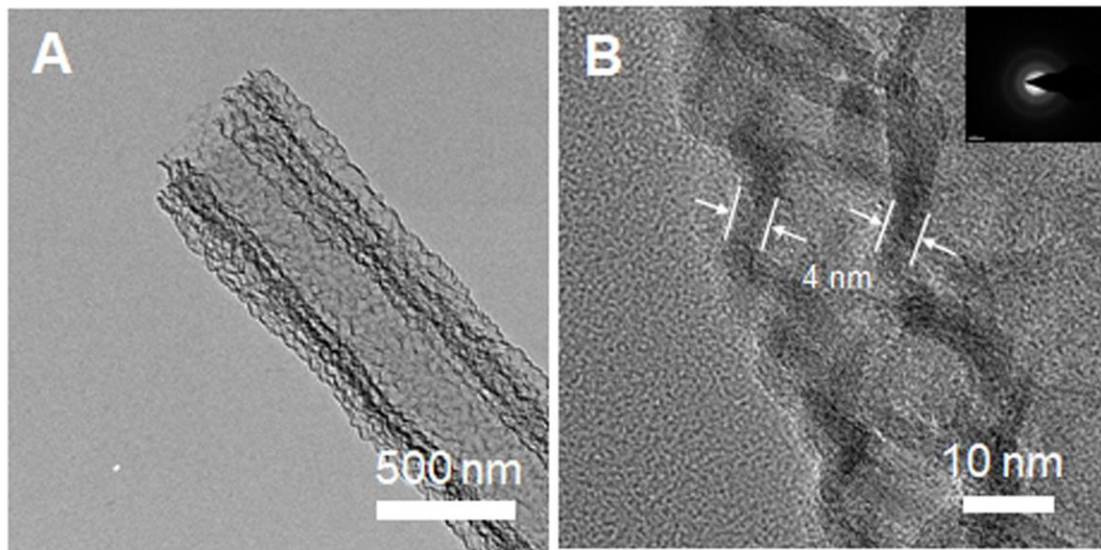
\*Correspondence to: morunwei@126.com, keningsunhit@126.com



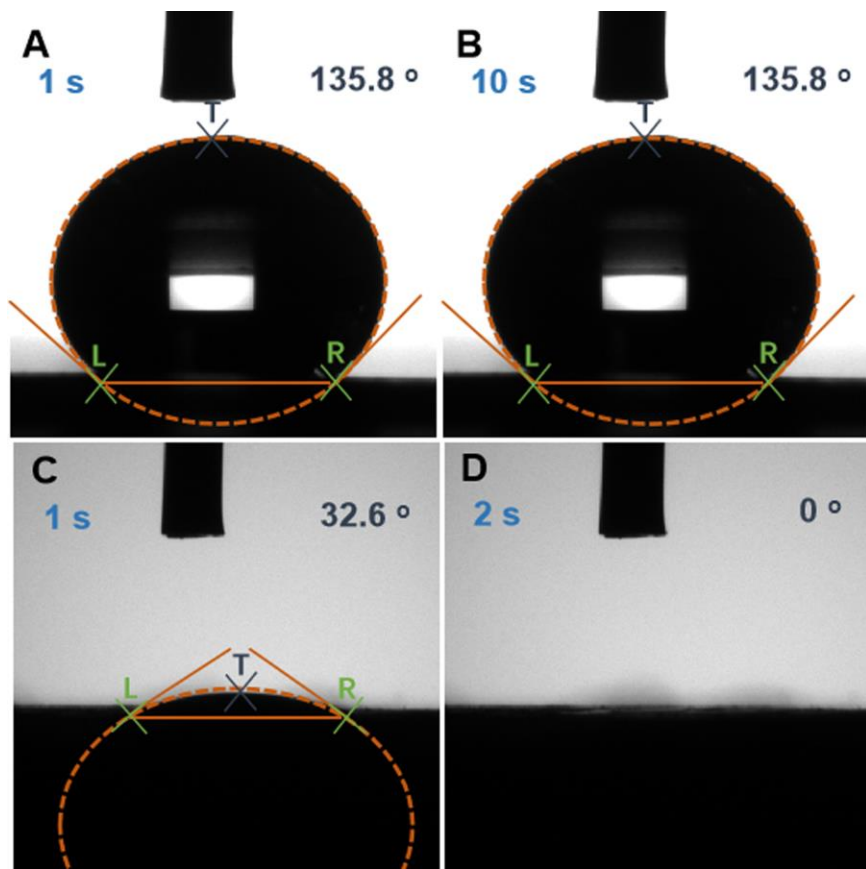
**Supplementary Figure 1.** (A) SEM image of the 3D-MgO rod. (B) SEM image of the 3D-MgO/N-doped graphene. (C) SEM image of the 3D-MgO/N-doped graphene/MgO. (D) SEM image of the 3D-MgO/N-doped graphene/MgO/graphene.



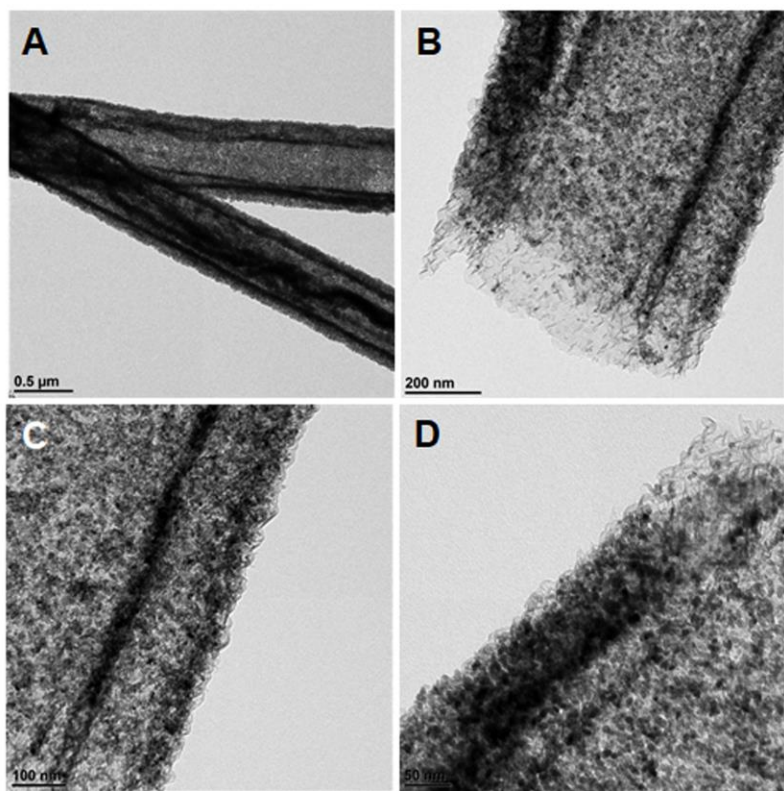
**Supplementary Figure 2.** Morphology characterization of the 3D-DHGT. (A,B) SEM images of the 3D-DHGT.



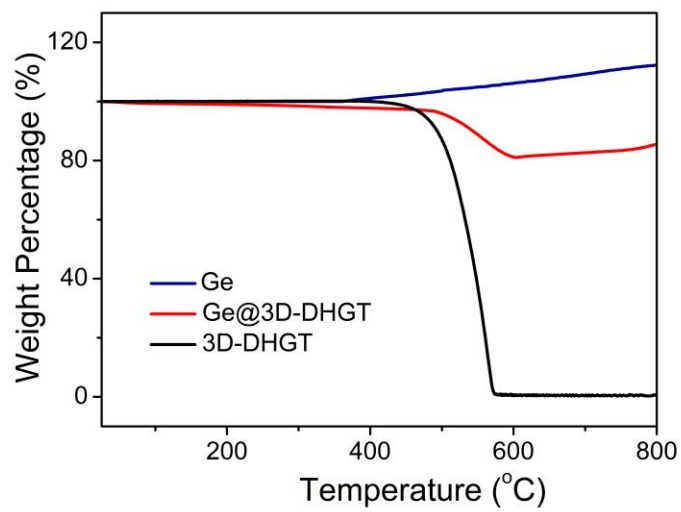
**Supplementary Figure 3.** (A,B) TEM images of the 3D-DHGT. The inset in (B) is the electronic diffraction pattern corresponding to the 3D-DHGT.



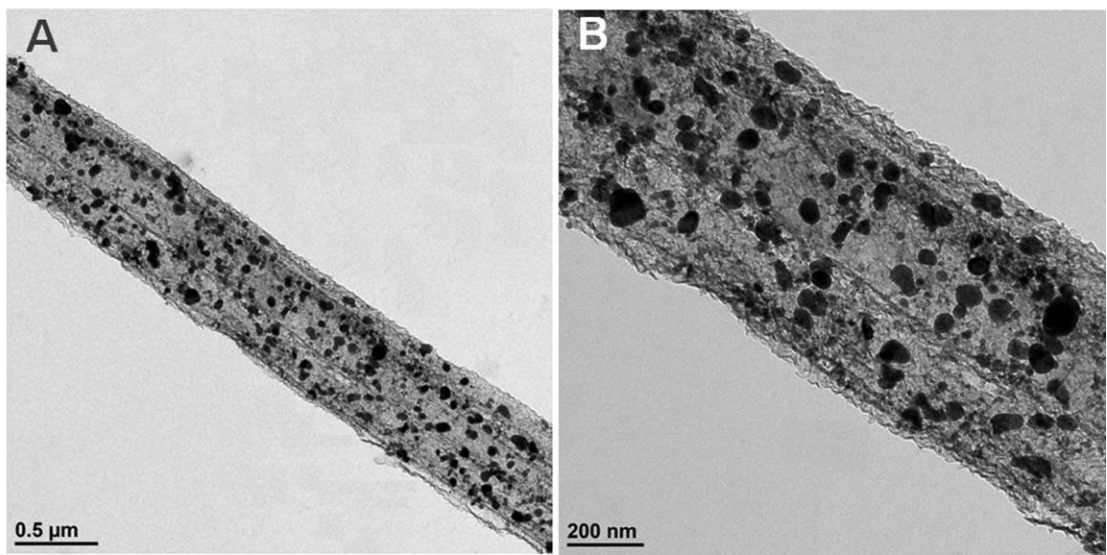
**Supplementary Figure 4.** (A-D) Variation of water CA over time (A,B) on the surfaces of outer graphene layer and (C,D) on the surfaces of inner N-doped graphene layer.



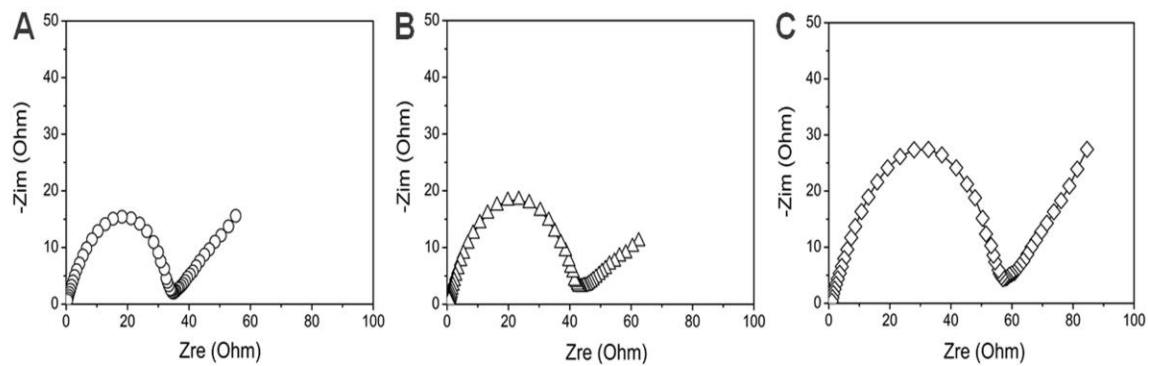
**Supplementary Figure 5.** (A-D) TEM images of the  $\text{GeO}_2$ @3D-DHGT.



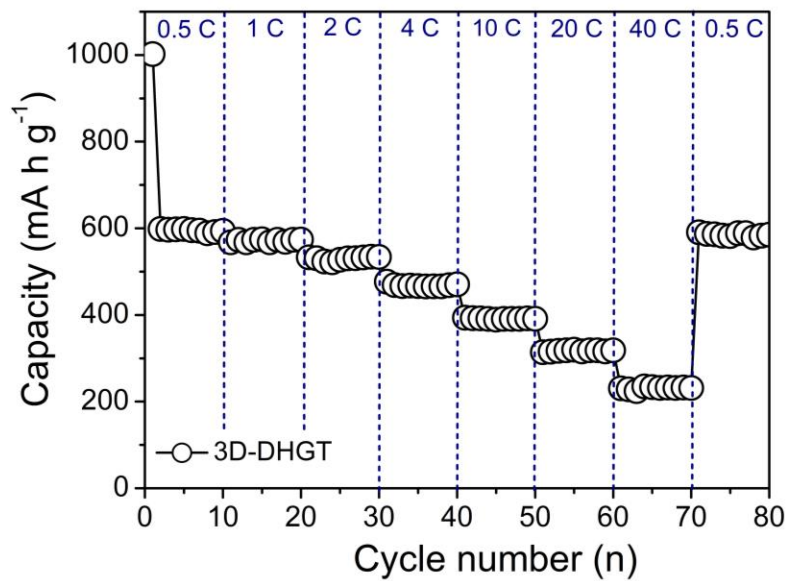
**Supplementary Figure 6.** TGA curves of Ge, 3D-DHGT, and  $\text{GeO}_2$ @3D-DHGT in air at a heating rate of  $5\text{ }^{\circ}\text{C min}^{-1}$ .



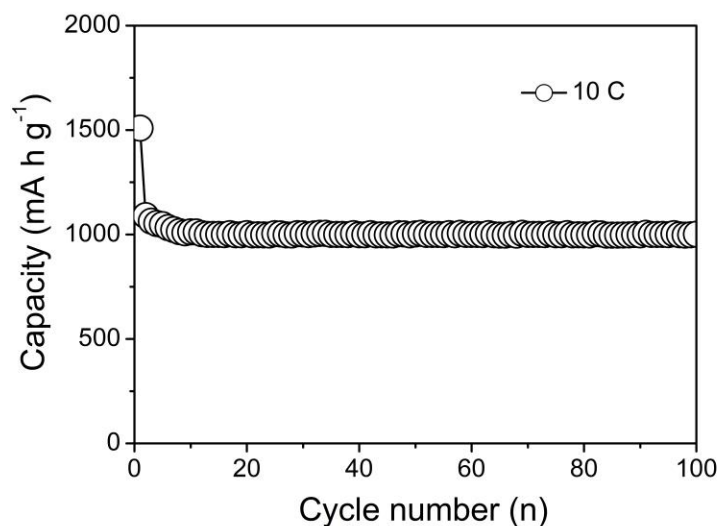
**Supplementary Figure 7.** TEM images of the Ge@3D-DHGT electrode after 1000 cycles at a rate of 0.5 C.



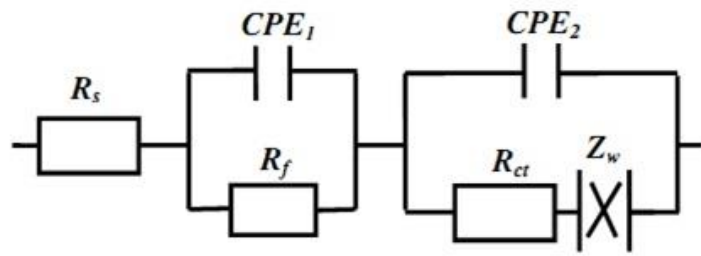
**Supplementary Figure 8.** Nyquist plots of Ge@3D-DHGT electrodes (a) before cycling, (b) after 100 cycles, and (c) after 1000 cycles.



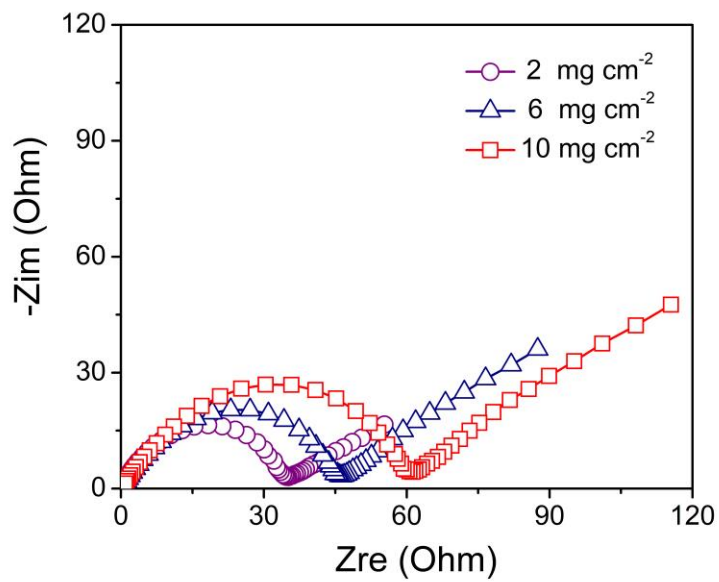
**Supplementary Figure 9.** Rate performance of the 3D-DHGT electrode at different current densities from 0.5 C to 40 C.



**Supplementary Figure 10.** Cycling performance (discharge) of Ge@3D-DHGT electrode with a mass loading of 2 mg cm<sup>-2</sup> at 10 C for 100 cycles.



**Supplementary Figure 11.** The equivalent circuit for the impedance behavior of the electrode.



**Supplementary Figure 12.** Nyquist plots of Ge@3D-DHGT electrodes under different mass loadings ( $2 \text{ mg cm}^{-2}$ ,  $6 \text{ mg cm}^{-2}$ , and  $10 \text{ mg cm}^{-2}$ ).

**Supplementary Table S1.** Mass ratio of Ge and 3D-DHGT at different temperature.

|        | 3D-DHGT<br>(wt%) | Ge<br>(wt%) | Ge@3D-DHGT<br>(wt%) | Ge:3D-DHGT<br>(mass ratio) |
|--------|------------------|-------------|---------------------|----------------------------|
| 600 °C | 0.10             | 106.54      | 82.22               | 77.80: 22.20               |
| 625 °C | 0.09             | 106.89      | 82.57               | 77.23: 22.77               |
| 650 °C | 0.06             | 107.67      | 82.93               | 77.01: 22.99               |

|        |      |        |       |             |
|--------|------|--------|-------|-------------|
| 700 °C | 0.06 | 108.42 | 83.31 | 76.83:23.17 |
|--------|------|--------|-------|-------------|

The residual weight percentage of 3D-DHGT, Ge, and the Ge@3D-DHGT at 600, 625, 650 and 675 °C are used to calculate the mass ratio of Ge and 3D-DHGT in the Ge@3D-DHGT composite. The weight of Ge increased during high temperature zone because the formation of  $\text{GeO}_x$ , meanwhile the weight of graphene decreased during the heat treatment owing to the decompose of graphene. Hence, we can use this equation to calculate the mass ratio of Ge and 3D-DHGT:

$$W_{\text{3D-DHGT}}(1-X_{\text{Ge}}) + W_{\text{Ge}}X_{\text{Ge}} = W_{\text{Ge@3D-DHGT}}$$

Where  $W_{\text{3D-DHGT}}$ ,  $W_{\text{Ge}}$ ,  $W_{\text{Ge@3D-DHGT}}$  are the residual weight percentage of 3D-DHGT, Ge and Ge@3D-DHGT at different temperature, respectively,  $X_{\text{Ge}}$  is the mass ratio of Ge in the composite. The mass ratio is listed in the table S1, which is quite stable at different temperature, and the average mass ratio of Ge and 3D-DHGT in the composite is 77.22% of Ge and 22.78% of 3D-DHGT.

**Supplementary Table S2.** A comparison of the cycle and rate performance of various Ge-based composites prepared by different structure designs.

| Materials                                | Carbon black (%) | Mass loading ( $\text{mg cm}^{-2}$ ) | Low Current Rate (C) | Capacity ( $\text{mA h g}^{-1}$ ) | High Current Rate (C) | Capacity ( $\text{mA h g}^{-1}$ ) | Reference |
|--|------------------|--------------------------------------|----------------------|-----------------------------------|-----------------------|-----------------------------------|-----------|
| 3D Macroporous Ge Particle               | 10               | 1.08                                 | 0.2                  | 1436                              | 5                     | 717                               | [1]       |
| Mesoporous Ge Particles                  | 15               | NA                                   | 0.2                  | 1350                              | 5                     | 804                               | [2]       |
| Carbon-Encapsulated Ge Nanowires         | 5                | NA                                   | 0.2                  | 1428                              | 10                    | 792                               | [3]       |
| Graphite Tubes-Encapsulated Ge Nanowires | 20               | 0.5                                  | 0.15                 | 1310                              | 7                     | 232                               | [4]       |
| Ge-Graphene-Carbon Nanotube Composite    | 10               | 0.7                                  | 0.1                  | 1277                              | 2                     | 754                               | [5]       |

|  |    |      |      |      |    |      |           |
|--|----|------|------|------|----|------|-----------|
| Graphene-Coating Ge Nanowires                            | 15 | 1.9  | 0.3  | 1300 | 20 | 363  | [6]       |
| Carbon Nanofibers-Encapsulated Ge Nanoparticles          | 0  | 0.5  | 0.15 | 1420 | 15 | 480  | [7]       |
| Flexible Carbon-Coated Ge Nanowires on Carbon Nanofibers | 0  | 1.2  | 0.1  | 1400 | 10 | 484  | [8]       |
| Ge@C/rGO Hybrids   | 10 | 1    | 0.1  | 1258 | 20 | 712  | [9]       |
| N-Doped Carbon with Embedded Ge Nanoparticles            | 0  | 2.24 | 0.1  | 1450 | 15 | 803  | [10]      |
| Polycrystalline Ge Microwire Film                        | 0  | NA   | 0.1  | 1350 | 1  | 1000 | [11]      |
| Core-Shell Ge@Graphene@TiO <sub>2</sub> Nanofibers       | 0  | 3.2  | 0.1  | 1150 | 2  | 760  | [12]      |
| Cu/Si/Ge NW Arrays Grown on Ni Foam                      | 0  | 1.2  | 1    | 2373 | 16 | 1010 | [13]      |
| Nanoporous Ge Nanofibers                                 | 15 | 1    | 0.2  | 1200 | 30 | 200  | [14]      |
| Ge@3D-DHGT   | 0  | 2    | 0.5  | 1338 | 40 | 752  | This work |
|  |    | 6    |      | 1121 | 20 | 536  |           |
|  |    | 10   |      | 1001 | 20 | 345  |           |

**Supplementary Table S3.** Impedance parameters calculated from equivalent circuit.

|            | R <sub>s</sub> (Ω) | R <sub>f</sub> (Ω) | R <sub>ct</sub> (Ω) |
|------------|--------------------|--------------------|---------------------|
| Ge/Cu      | 6                  | 62                 | 25                  |
| Ge@3D-DHGT | 3                  | 29                 | 11                  |

## References

1. Jia, H. P.; Kloepsch, R.; He, X.; Badillo, J. P.; Gao, P. F.; Fromm, O.; Placke, T.; Winter, M. Reversible Storage of Lithium in Three-Dimensional Macroporous Germanium. *Chem. Mater.* **2014**, *26*, 5683–5688.
2. Choi, S.; Kim, J.; Choi, N. S.; Kim, M. G.; Park, S. Cost-Effective Scalable Synthesis of Mesoporous Germanium Particles via a Redox-Transmetalation Reaction for High-Performance Energy Storage Devices. *ACS Nano.* **2015**, *9*, 2203–2212.
3. Liu, J.; Song, K. P.; Zhu, C. B.; Chen, C. C.; Aken, P. A.; Maier, J.; Yu, Y. Ge/C Nanowires as High-Capacity and Long-Life Anode Materials for Li-Ion Batteries. *ACS Nano.* **2014**, *8*, 7051–7059.
4. Sun, Y.; Jin, S. X.; Yang, G. W.; Wang, J.; Wang, C. X. Germanium Nanowires-In-Graphite Tubes via Self-Catalyzed Synergetic Confined Growth and Shell-Splitting Enhanced Li-Storage Performance. *ACS Nano.* **2015**, *9*, 3479–3490.
5. Fang, S.; Shen, L. F.; Zheng, H.; Zhang, X. G. Ge-Graphene-Carbon Nanotube Composite Anode for High Performance Lithium-Ion Batteries. *J. Mater. Chem. A.* **2015**, *3*, 1498–1503.
6. Kim, H.; Son, Y. K.; Park, C.; Cho, J.; Choi, H. C. Catalyst-Free Direct Growth of A Single to A Few Layers of Graphene on A Germanium Nanowire for The Anode Material of A Lithium Battery. *Angew. Chem. Int. Ed.* **2013**, *52*, 5997–6001.
7. Li, W. H.; Yang, Z. Z.; Cheng, J. X.; Zhong, X. W.; Gu, L.; Yu, Y. Germanium Nanoparticles Encapsulated in Flexible Carbon Nanofibers as Self-Supported Electrodes for High Performance Lithium-Ion Batteries. *Nanoscale.* **2014**, *6*, 4532–4537.

8. Li, W. H.; Li, M. S.; Yang, Z. Z.; Xu, J.; Zhong, X. W.; Wang, J. Q.; Zeng, L. C.; Liu, X. W.; Jiang, Y.; Wei, X.; Gu, L.; Yu, Y. Carbon-Coated Germanium Nanowires on Carbon Nanofibers as Self-Supported Electrodes for Flexible Lithium-Ion Batteries. *Small*. **2015**, *11*, 2762–2767.
9. Wang, B. R.; Wen, Z. Y.; Jin, J.; Hong, X. H.; Zhang, S. P.; Rui, K. A Novel Strategy to Prepare Ge@C/rGO Hybrids as High-Rate Anode Materials for Lithium Ion Batteries. *J. Power Sources*. **2017**, *342*, 521–528.
10. Ma, X. M.; Zhou, Y. N.; Chen, M.; Wu, L. M. Synthesis of Olive-Like Nitrogen-Doped Carbon with Embedded Ge Nanoparticles for Ultrahigh Stable Lithium Battery Anodes. *Small*. **2017**, *13*, 1700403.
11. Ma, L. Y.; Fahrenkrug, E.; Gerber, E.; Crowe, A. J.; Venable, F.; Bartlett, B. M.; Maldonado, S. High-Performance Polycrystalline Ge Microwire Film Anodes for Li Ion Batteries. *ACS Energy Lett.* **2017**, *2*, 238–243.
12. Wei, W.; Wang, H.; Tian, A. H.; Wang, K. F.; Wang, J. M.; Qu, P.; Zhang, S. Y.; Guo, L. Confined Metal Ge Quantum Dots in Carbon Nanofibers for Stable Rechargeable Batteries. *Nanoscale*. **2018**, *10*, 6872–6877.
13. Zhang, Q. B.; Chen, H. X.; Luo, L. L.; Zhao, B. T.; Luo, H.; Han, X.; Wang, J. W.; Wang, C. M.; Yang, Y.; Zhu, T.; Liu, M. L. Harnessing the Concurrent Reaction Dynamics in Active Si and Ge to Achieve High Performance Lithium-Ion Batteries. *Energy Environ. Sci.* **2018**, *11*, 669–681.
14. Kim, C.; Song, G.; Luo, L. L.; Cheong, J. Y.; Cho, S. H.; Kwon, D.; Choi, S.; Jung, J. W.; Wang, C. M.; Kim, I.; Park, S. Stress-Tolerant Nanoporous Germanium Nanofibers for Long Cycle Life Lithium Storage with High Structural Stability. *ACS Nano*. **2018**, *12*, 8169–8176.